Spectral statistics in the quantized cardioid billiard

A. Bäcker* and F. Steiner

*II. Institut für Theoretische Physik, Universität Hamburg, Luruper Chaussee 149,
22761 Hamburg, Federal Republic of Germany*

P. Stifter†

Abteilung für Quantenphysik, Universität Ulm, 89069 Ulm, Federal Republic of Germany

The spectral statistics of the strongly chaotic cardioid billiard is studied. The analysis is based on the first 11 000 quantal energy levels for both odd and even symmetry. It is found that the level-spacing distribution is in good agreement with the Gaussian-orthogonal-ensemble distribution of random-matrix theory. In the cases of the number variance and rigidity we observe agreement with the random-matrix model for short-range correlations only, whereas for long-range correlations both statistics saturate in agreement with semiclassical expectations. Furthermore the conjecture that for classically chaotic systems the normalized mode fluctuations have a universal Gaussian distribution with unit variance is tested and found to be in very good agreement for both symmetry classes. By means of the Gutzwiller trace formula the trace of the cosine-modulated heat kernel is studied. Since the billiard boundary is focusing, there are conjugate points that give rise to zeros instead of exclusively at Gaussian peaks at the locations of the periodic orbits.

PACS number(s): 05.45.+b, 03.65.Sq

I. INTRODUCTION

Today the important role played by chaos in nonlinear dynamical systems is generally appreciated. The most striking property of deterministic chaos is the sensitive dependence on initial conditions such that neighboring trajectories in phase space separate at an exponential rate. As a result the long-time behavior of a strongly chaotic system is unpredictable. There the fundamental question arises whether this well-established phenomenon of classical chaos has an analogue in the quantum world that could be called "quantum chaos." By this the following is meant: Given a dynamical system which is strongly chaotic, i.e., ergodic, mixing, and a K system, is there any manifestation in the corresponding quantal system which betrays its chaotic character? (For an authoritative review, see Ref. [1].) If one were to identify unique fingerprints of classical chaos in quantum mechanics, one could use these to *define* quantum chaos. Ideally, classically chaotic systems should be characterized by a random behavior of these fingerprints that qualify the system to be called "chaotic" also in quantum mechanics.

For bound conservative systems, the quantum mechanical time evolution is almost periodic, in the sense of Harald Bohr's theory of almost periodic functions, due to the discrete spectrum of the time-evolution operator. One thus observes no sensitive dependence on initial conditions in the long-time behavior of quantum mechanics. This is in contrast to classical systems whose time evolution is ruled by the Liouville operator. If the classical dynamics is strongly chaotic, the spectrum of the Liouvillian has a continuous spectrum on the unit circle which leads to a decay of time correlations of classical observables reflecting a complete loss of information on the system. This fundamental difference between classical and quantum mechanics has led to the common belief that there hardly exists any phenomenon in quantum mechanics which justifies the notion of quantum chaos.

However, instead of concentrating on the long-time behavior, one can consider the extreme limit $t = \infty$ in quantum mechanics and thus study properties of stationary states, that is, of eigenvalues and eigenfunctions of the corresponding time-independent Hamiltonian. The idea is that the statistical properties of the energy-level fluctuations ("spectral statistics") and wave functions of a given quantum system are already determined by its classical limit, depending only upon whether this limit is chaotic or not. (In this paper we shall consider the spectral statistics only; for a discussion of the statistical properties of wave functions in chaotic systems, see Refs. [1–6].) It has been conjectured that the statistical properties of quantum energy spectra of classically integrable systems can be described [7] by Poissonian random processes, whereas the spectral statistics of strongly chaotic systems can be described [8] by the universal laws of random-matrix theory (RMT), originally proposed by Wigner, and Landau and Smorodinsky, and fully developed by Dyson for a better understanding of the resonances of compound nuclei. (See Ref. [9] for a collection of the original papers, and Refs. [1,10,11] for recent reviews.) The *random-matrix model* for spectral statistics has to be viewed as a purely phenomenological one, in contrast to random-matrix theory which constitutes an exact mathematical theory. So far there does not exist a complete theory for the spectral statistics of chaotic sys-

*Electronic address: baeckera@x4u2.desy.de
†Electronic address: stif@physik.uni-ulm.de

tems, nor even for integrable ones. Based on Gutzwiller's trace formula [12,1], Berry carried out a semiclassical analysis [13-15] of the level fluctuations and obtained a saturation of the two-point statistics for long-range correlations in contradiction with the predictions based on RMT; nonuniversal long-range correlations occur due to the nonuniversal behavior of short periodic orbits. A recent analysis [16,17] based on the exact Selberg trace formula has clearly confirmed the nonuniversal saturation up to correlation lengths as large as $L = 700$ (in units of the average level spacing). In addition, there exists a class of strongly chaotic systems for which the spectral fluctuations nearly behave as is expected for classically integrable systems. This phenomenon occurs for geodesic flows on hyperbolic manifolds (for instance, Riemannian surfaces with constant negative Gaussian curvature), whose fundamental groups are of an arithmetical origin; thus the notion of arithmetical chaos was introduced [18,19]. The dynamical systems possessing arithmetical chaos violate universality in energy-level statistics even in the short-range regime. It thus appears that the random-matrix model does not provide a universal signature of classical chaos in quantum mechanics.

Recently, a novel quantity to measure quantum chaos has been proposed and a conjecture about its statistical behavior has been put forward [5,17]. According to this conjecture there are unique fluctuation properties in quantum mechanics which are *universal* and, in a well-defined sense, *maximally random* if the corresponding classical system is strongly chaotic. Numerical as well as theoretical evidence has been provided in favor of the conjecture [6,17]. A rigorous proof of the conjecture would give us a clear-cut definition of *quantum chaos in spectra*.

In order to shed more light on the relationship between classically chaotic systems and the corresponding quantum systems it is important to have a large number of systems for which it is possible to carry out extensive numerical computations of the relevant spectral statistics. The simplest nonlinear dynamical systems one can study are billiard systems. They consist of a point particle moving freely inside a curved boundary with elastic reflections at the boundary. These systems are specially suited for the study of a possible manifestation of classical chaos in quantum mechanics, because a lot of mathematical results are available. Furthermore the integration of the equations of motion is trivial, i.e., the geodesics are straight lines, which by no means implies that it is trivial to determine all periodic orbits having periods below a given value. Moreover, billiard systems belong to the so-called scaling systems with the semiclassical limit of Planck's constant $\hbar \to 0$ being equivalent to the high energy limit $E \to \infty$.

In this paper we are concerned with a billiard system bounded by the cardioid. This system is of special interest because it provides one of the few examples for which it is rigorously proven that it is strongly chaotic [21-24]. Famous other examples are the Sinai billiard [25,26], which is very important for the foundations of statistical mechanics, and Bunimovich's stadium billiard [27-30]. However, the last two systems possess some non-generic features, because they have a family of stable

periodic orbits, the so-called bouncing-ball modes. The cardioid billiard has no such family, and no whispering gallery orbits exist. Furthermore the boundary is focusing and the geometric properties are such that caustics exist. Their important influence will become clear in Sec. IV in the discussion of the cosine-modulated heat kernel.

The paper is organized as follows. After defining the cardioid billiard and its quantum mechanical version in Sec. II, we present in Secs. III A to III E a detailed analysis of the spectral statistics, i.e., the spectral staircase function, the δ_n statistics, the level-spacing distribution $P(s)$, the number variance $\Sigma^2(L)$, and the rigidity $\Delta_3(L)$. In Sec. III F the distribution of the mode-fluctuation number is calculated and found to be in excellent agreement with the recent conjecture [5,6] on quantum chaos in spectra. In order to keep the number of figures limited, the various spectral measures are displayed in each case for one symmetry class only, but we show the plots for even and odd symmetry in an alternating order. In Sec. IV we consider the trace of the cosine-modulated heat kernel as an additional test of the accuracy of the eigenvalues and as a first application of Gutzwiller's periodic-orbit theory. Section V contains a summary and discussion of our results.

II. THE CARDIOID BILLIARD

The billiard system to be studied is given by the free motion of a point particle inside a two-dimensional Euclidean domain Ω bounded by the cardioid (see Fig. 1) with elastic reflections at the boundary $\partial\Omega$. The cardioid billiard is the limit case of a family of billiards which was introduced by Robnik [20]. The boundary $\partial\Omega$ of the billiards is defined by a quadratic conformal mapping of the unit circle

$$w = u + iv = z + \lambda z^2;$$

$$z = e^{i\varphi}, \quad \varphi \in [0, 2\pi[, \quad \lambda \in [0, \tfrac{1}{2}[\quad . \quad (1)$$

Starting with $\lambda = 0$ one gets a continuous deformation of the circle. The cardioid billiard is obtained for $\lambda = \frac{1}{2}$; for this value the mapping is no longer conformal, since $\frac{dw}{dz} = 1 + z = 0$ for $z = -1$ ($\varphi = \pi$), where the cardioid has a cusp. It was proven that the cardioid billiard is ergodic, mixing, and a K system [21-23]. In fact it is even
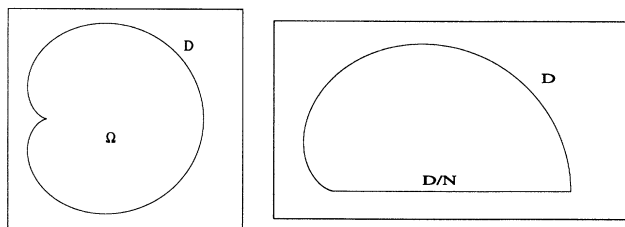

FIG. 1. Full and desymmetrized cardioid billiard. D denotes Dirichlet and N Neumann boundary conditions.

a Bernoulli system, which follows from a recent result [24]. The corresponding quantum mechanical system is governed by the Schrödinger equation (in natural units $\hbar = 2m = 1$)

$$-\Delta \Psi_n(\vec{q}) = E_n \Psi_n(\vec{q}), \quad \vec{q} \in \Omega \ ,$$

with Dirichlet condition $\Psi_n(\vec{q}) = 0$ at the boundary $\partial \Omega$. Δ is the two-dimensional Laplacian. Furthermore, we have the orthonormality relation

$$\int_\Omega d^2 q \, \Psi_m(\vec{q}) \, \Psi_n(\vec{q}) = \delta_{mn} \ .$$

Notice that the eigenfunctions $\Psi_n(\vec{q})$ can be chosen as real. For Ω being compact the energy spectrum $\{E_n\}$ is purely discrete. Since the system is invariant under reflection at the symmetry line ($v = 0$) one can classify the wave functions $\Psi_n(\vec{q})$ as odd and even eigenfunctions satisfying Dirichlet or Neumann boundary conditions respectively at the symmetry line. Therefore we will consider the two desymmetrized versions of the cardioid billiard only; see Fig. 1.

For the following discussion it is important to keep in mind that the semiclassical limit $\hbar \to 0$ corresponds to the high energy limit $E_n \to \infty$.

III. SPECTRAL STATISTICS

A. Spectral staircase and Weyl's law

One can easily check the asymptotic behavior of the spectrum by calculating the spectral staircase function (integrated level density)

$$N(E) = \mathcal{N}(\{n | E_n < E\}) \ , \tag{2}$$

which counts the number of energy levels below E. $N(E)$ can be divided into a smooth and an oscillatory part

$$N(E) = \bar{N}(E) + N_{\mathrm{osc}}(E) \ .$$

The mean behavior of $N(E)$ is asymptotically for $E \to \infty$ described by the generalized Weyl's law including perimeter, corner, and curvature corrections [31]. For odd ($-$) and even ($+$) symmetry, respectively, one obtains

$$\bar{N}^-(E) = \frac{3}{16} E - \frac{3}{2\pi} \sqrt{E} + \frac{3}{16} \ , \tag{3}$$

$$\bar{N}^+(E) = \frac{3}{16} E - \frac{1}{2\pi} \sqrt{E} \ , \tag{4}$$

where the inward pointing cusp contributes like an edge with angle π in the desymmetrized billiard. In Fig. 2 the spectral staircase $N^-(E)$ is shown for the first 11 000 energy levels for odd symmetry and compared with the generalized Weyl's law $\bar{N}^-(E)$, Eq. (3). Due to the large energy interval no difference between both curves is visible in this figure on the whole range. Therefore two insets at the lowest and highest ends are shown. The
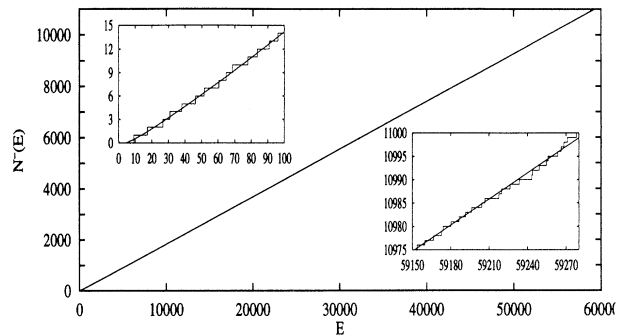

FIG. 2. Spectral staircase $N^-(E)$ for odd symmetry and generalized Weyl's law, Eq. (3). The insets show a magnification of the energy intervals $[0, 100]$ and $[59\,150, 59\,270]$ respectively.

eigenvalues were computed by Prosen and Robnik [32] by using the conformal mapping diagonalization technique which was introduced by Robnik [33,34]. In Ref. [34] the energy-level statistics was investigated in detail for the family of billiards (1) for various parameters $\lambda < \frac{1}{2}$ for which a rigorous proof of strong chaos is lacking.

Despite the fact that $\bar{N}^-(E)$ is an asymptotic law, it gives the correct mean behavior down to the ground state, as was observed in many other systems before. Figure 2 strongly indicates that the computed energy spectrum for odd symmetry is complete for the first 11 000 levels. In the same way we have also checked the energy spectrum for even symmetry being complete for the first 11 000 levels. Furthermore, no degeneracies of eigenvalues in the spectra for even and odd symmetry were found.

In order to compare the eigenvalues of the cardioid billiard with those of other systems, it is necessary to unfold the spectrum by means of the generalized Weyl's law (3) or (4)

$$E_n'^{\pm} = \bar{N}^{\pm}(E_n^{\pm}) \ .$$

In the following we shall analyze the unfolded spectra $\{E_n'^{\pm}\}$ for the two desymmetrized billiards, but the prime and superscript $\pm$ will be omitted. After the process of unfolding the spectrum has a mean level spacing of unity, and different systems differ in the oscillating part $N_{\mathrm{osc}}(E)$ only.

B. δ_n statistics

A more refined way of testing whether the spectrum is complete can be performed by considering the fluctuating part $N_{\mathrm{osc}}(E_n)$ of the spectral staircase function evaluated [35] at the unfolded eigenvalues E_n

$$\delta_n := N_{\mathrm{osc}}(E_n) := N(E_n) - \bar{N}(E_n) = n - \tfrac{1}{2} - E_n \ . \tag{5}$$

As one can see in Fig. 3, where the even case is shown, δ_n is oscillating around zero, showing that the levels indeed obey the mean behavior as described by Weyl's law. If a level was missing, δ_n would oscillate around -1 from then
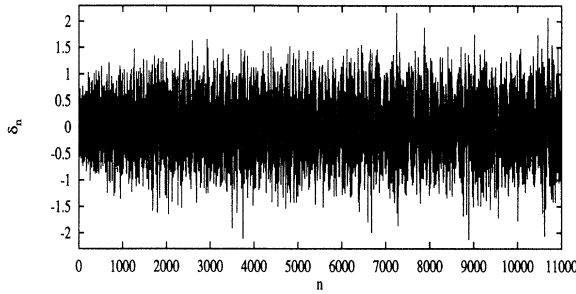
FIG. 3. Plot of the fluctuating part $\delta_n := N_{\text{osc}}(E_n)$ $:= n - \frac{1}{2} - E_n$ for even symmetry for the first 11 000 eigenvalues.

on. This indicates that the spectrum for even symmetry is complete for the first 11 000 levels. The same holds for the odd case.

Remarkably, the δ_n statistics is even sensitive to the constant term in Weyl's law, Eqs. (3) and (4), as one can infer from the mean values of δ_n for which we obtain $\langle \delta \rangle = -0.000\,72$ for odd and $\langle \delta \rangle = -0.002\,17$ for even symmetry. This is in the odd case more than a factor 200 less than the constant $C_{\text{odd}} = \frac{3}{16} = 0.1875$ in Eq. (3). In case of the constant being neglected or unknown, the mean value of δ_n would provide a good approximation to the constant term in Weyl's law.

Although the fluctuations δ_n have mean zero, a look at Fig. 3 suggests that their variance slowly increases with increasing energy. A quantitative discussion of this important observation will be postponed until Sec. III E.

C. Level-spacing distribution

An important statistic measuring short-range correlations of the spectrum is the nearest-neighbor level-spacing statistic $P(s)$. $P(s)\,ds$ is the probability of finding an arbitrary pair of nearest neighbors of energy levels with spacing $s_n = E_{n+1} - E_n$ in the interval $[s, s + ds]$. Thus $P(s)$ measures fluctuations of the distances between two nearest-neighbor levels.

The level-spacing distribution for typical integrable systems is found to obey the Poissonian distribution $P^{\text{Pois}}(s) = e^{-s}$, which is in clear contrast to the level repulsion observed in generic chaotic systems. The random-matrix model [10] predicts that for systems with time-reversal symmetry the level-spacing distribution $P(s)$ is given by the distribution of the Gaussian orthogonal ensemble (GOE) which is well described by a Wigner distribution

$$P^{\text{GOE}}(s) = \frac{\pi}{2} s \exp\left\{-\frac{\pi}{4}s^2\right\} \ ,$$

whereas systems without such symmetry should obey the distribution of the Gaussian unitary ensemble (GUE) which is in good approximation given by

$$P^{\text{GUE}}(s) = \frac{32}{\pi^2} s^2 \exp\left\{-\frac{4}{\pi}s^2\right\} \ .$$
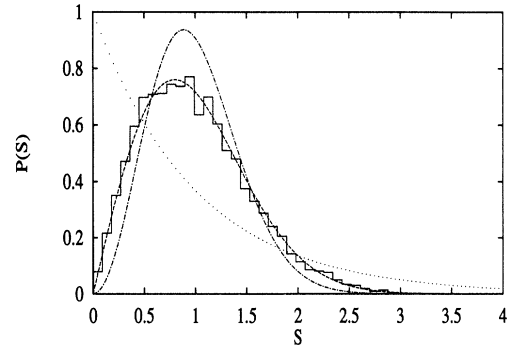

FIG. 4. Histogram of the nearest-neighbor level-spacing distribution $P(s)$ for odd symmetry. The dashed line is the expected Wigner distribution, the dashed-dotted line is the GUE distribution, and the dotted line shows the Poissonian distribution expected for integrable systems.

Since the cardioid billiard possesses time-reversal symmetry the level-spacing distribution is expected to be described by a Wigner distribution. In Fig. 4 the level-spacing distribution for odd symmetry is shown. The agreement with $P^{\text{GOE}}(s)$ is very good. A similar result holds in the even symmetry case.

The level-spacing distribution has the drawback that there is a loss of information due to the binning. Therefore it is more significant to look at the cumulative level-spacing distribution

$$I(s) = \int_0^s P(s')\,ds' \ .$$

Numerically this quantity is calculated by sorting the set of nearest-neighbor spacings $\{s_n\}$ and determining the fraction of level spacings below a given s.

As one can see in Fig. 5, where the even case is shown, the agreement between the cumulative level-spacing distribution and the cumulative GOE expectation is very
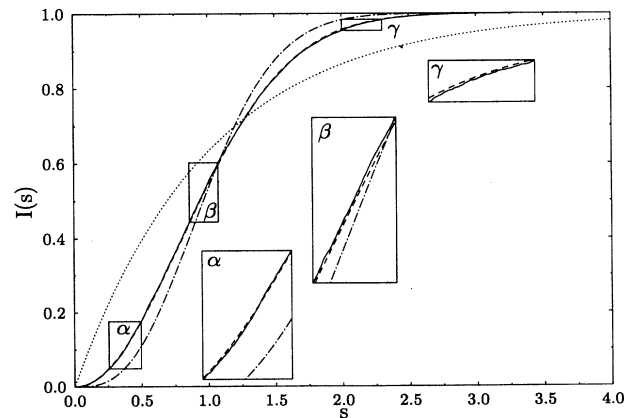

FIG. 5. Cumulative level spacing for even symmetry. Full line: calculated from the energy levels; dashed line: GOE expectation $I^{\text{GOE}}(s)$; dashed-dotted line: GUE expectation $I^{\text{GUE}}(s)$; and dotted line the Poissonian distribution $I^{\text{Pois}}(s)$.

good. The Kolmogorov-Smirnov test gives a significance level of $\mathcal{P} = 24\%$ for the odd and $\mathcal{P} = 67\%$ for the even case assuming a GOE distribution, whereas for the GUE distribution an extremely small significance level of $\mathcal{P} < 10^{-52}$ is obtained for both symmetry classes.

D. Number variance

In contrast to the level-spacing statistic, the number variance allows one to investigate also medium- and long-range correlations of the spectrum. It is defined by

$$\Sigma^2(L, \hat{E}) := \left\langle [n(L, E) - L]^2 \right\rangle_{\hat{E}, \delta}, \quad L > 0 \ ,$$

which is the local variance of the number $n(L, E) = N(E + \frac{L}{2}) - N(E - \frac{L}{2})$ of unfolded energy levels E_n in the interval $[E - \frac{L}{2}, E + \frac{L}{2}]$. The angular brackets $\langle \rangle_{\hat{E}, \delta}$ denote a local average with center $\hat{E}$ and effective width δ. Different averaging procedures are possible; here we have chosen a rectangular averaging

$$\langle f(E) \rangle_{\hat{E}, \delta} = \frac{1}{\delta} \int_{\hat{E} - \delta/2}^{\hat{E} + \delta/2} f(E) \, dE \ . \tag{6}$$

In random-matrix theory one obtains in the GOE case

$$\Sigma^2_{\text{GOE}}(L) = \frac{2}{\pi^2} \left\{ \ln(2\pi L) + \gamma + 1 + \frac{1}{2}\text{Si}^2(\pi L) - \frac{\pi}{2}\text{Si}(\pi L) \right.$$
$$- \cos(2\pi L) - \text{Ci}(2\pi L)$$
$$\left. + \pi^2 L \left[1 - \frac{2}{\pi}\text{Si}(2\pi L) \right] \right\} \ , \tag{7}$$

and for the GUE

$$\Sigma^2_{\text{GUE}}(L) = \frac{1}{\pi^2} \left\{ \ln(2\pi L) + \gamma + 1 - \cos(2\pi L) \right.$$
$$\left. - \text{Ci}(2\pi L) + \pi^2 L \left[1 - \frac{2}{\pi}\text{Si}(2\pi L) \right] \right\} \ , \tag{8}$$

where $\text{Si}(x)$ and $\text{Ci}(x)$ are the sine and cosine integral, respectively, and $\gamma = 0.5772\ldots$ is Euler's constant. For a random Poissonian process one has

$$\Sigma^2_{\text{Pois}}(L) = L \ ,$$

which is in agreement with the general small-L behavior $\Sigma^2(L) = L + O(L^2)$, following from the fact that $N(E)$ is a staircase function.
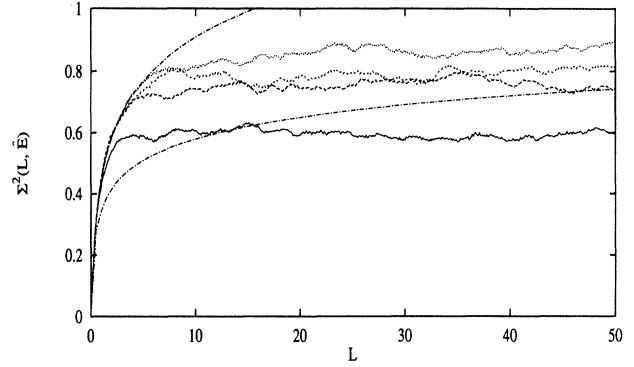

FIG. 6. Number variance $\Sigma^2(L, \hat{E})$ for odd symmetry at different energies $\hat{E}$: $\hat{E} = 1000$ (full line), 4000 (long dashed line), 7000 (short dashed line), 10 000 (dots); $\delta = 1800$. Upper dashed-dotted line: GOE expectation $\Sigma^2_{\text{GOE}}(L)$; lower dashed-dotted line: GUE expectation $\Sigma^2_{\text{GUE}}(L)$.

In Fig. 6 we show the number variance in the odd symmetry case for $L \leq 50$ and different values of $\hat{E}$: $\hat{E} = 1000, 4000, 7000, 10\,000$ ($\delta = 1800$). In Table I the saturation values $\Sigma^2_\infty(\hat{E})$, calculated as the average of $\Sigma^2(L, \hat{E})$ over $L \in [15, 100]$, are listed. It is seen that the agreement with the GOE expectation (dashed-dotted line) is restricted to $L \leq 2, \ldots, 7$, depending on $\hat{E}$. Analogous results hold in the even symmetry case.

It is now well established that the medium- and long-range statistics measured by the number variance strongly depend on the (nonuniversal) short periodic orbits [13–15,36,16,17]. Therefore the universality regime, which is expected to be governed by the random-matrix model, is restricted to very small correlation lengths L, which is confirmed by our numerical results. In order to enlarge the range of agreement with the random-matrix model, the center of the averaging window has to be in the deep semiclassical regime corresponding to extremely high lying energy levels. According to Berry's semiclassical analysis [14,15] $\Sigma^2_\infty(\hat{E})$ should increase with increasing energy $\hat{E}$ in the limit of large $\hat{E}$. A look at Fig. 6 and Table I shows that such an overall increase is indeed observed within the relatively large fluctuations of the number variance.

E. Spectral rigidity

Another statistic measuring two-point correlations is the spectral rigidity [10]

TABLE I. Saturation values $\Sigma^2_\infty(\hat{E})$ of the number variance and $\Delta_\infty(\hat{E})$ of the rigidity at different energies $\hat{E}$. Notice that the last digit is uncertain.

$\hat{E}$	$\Sigma^2_\infty(\hat{E})$ (odd)	$\Sigma^2_\infty(\hat{E})$ (even)	$\Delta_\infty(\hat{E})$ (odd)	$\Delta_\infty(\hat{E})$ (even)
1000	0.59	0.60	0.29	0.29
4000	0.75	0.75	0.38	0.37
7000	0.79	0.83	0.40	0.41
10 000	0.85	0.83	0.43	0.38

$$\Delta_3(L, \hat{E}) := \left\langle \min_{(a,b)} \frac{1}{L} \int_{-L/2}^{L/2} d\epsilon \, [N(E + \epsilon) - a - b\epsilon]^2 \right\rangle_{\hat{E}, \delta} ,$$

$$(9)$$

which is the average mean square deviation of the spectral staircase function from the best fitting straight line over an energy range of L mean level spacings. The angular brackets $\langle \rangle_{\hat{E}, \delta}$ again represent a local average.

For short correlation lengths $L \ll 1$ the rigidity is independent of the underlying spectrum, and obeys $\Delta_3(L) \sim \frac{1}{15}L$, which is a consequence of $N(E)$ being a staircase function.

In the theory of random matrices (RMT) $\Sigma^2(L)$ and $\Delta_3(L)$ are related through

$$\Delta_3^{\mathrm{RMT}}(L) = \frac{2}{L^4} \int_0^L \left(L^3 - 2L^2 r + r^3 \right) \Sigma_{\mathrm{RMT}}^2(r) \, dr .$$

$$(10)$$

By this equation it is possible to obtain $\Delta_3^{\mathrm{GOE}}(L)$ or $\Delta_3^{\mathrm{GUE}}(L)$ by numerical integration of Eqs. (7) or (8).

In Fig. 7 the rigidity calculated from Eq. (9) is shown for different energies $\hat{E}$ and $\delta = 1800$. One clearly observes a saturation effect of the rigidity for large L as is suggested by Berry's analysis [13] of the spectral rigidity using the semiclassical trace formula. This is in contrast to the logarithmic increase predicted by random-matrix theory; see Eq. (7). The rigidity is smoother than the number variance, but reaches the saturation later in comparison with $\Sigma^2(L, \hat{E})$. The prediction of the random-matrix model for the rigidity suffers from the same drawback as in the case of the number variance, i.e., that it is valid for small correlation lengths L only.

For the following section it is of great importance to know the dependence of the saturation value $\Delta_\infty(\hat{E})$ of the rigidity on the energy. $\Delta_\infty(\hat{E})$ is defined as $\Delta_\infty(\hat{E}) = \lim_{L \to \infty} \Delta_3(L, \hat{E})$. According to Berry's semiclassical analysis [13] one expects in the semiclassical

limit $\hat{E} \to \infty$ for systems with time-reversal symmetry

$$\Delta_\infty(\hat{E}) = \frac{1}{2\pi^2} \ln \hat{E} + C .$$

$$(11)$$

The constant C has been estimated by Berry as $C = C(l_0) = \frac{1}{\pi^2} \ln[4\pi e \bar{d}(\hat{E})/l_0] - \frac{1}{8}$ where $\bar{d}(\hat{E}) = \frac{d\bar{N}(\hat{E})}{d\hat{E}}$ is the mean level density, l_0 denotes the length of the shortest periodic orbit, and e is the base of the natural logarithm. In the case of the cardioid billiard we have $l_0 = 2.598 \ldots$ and thus obtain $C(l_0) \approx -0.034$ for both symmetry classes. Due to the finite number of available energy levels we cannot perform the limit $L \to \infty$. Therefore we have determined $\Delta_\infty(\hat{E})$ from a fit of $\Delta_3(L; \hat{E})$ in the range $L \in [15, 400]$ for fixed $\hat{E}$ to the function

$$\Delta_3^{\mathrm{fit}}(L) = \Delta_\infty \left(1 + \frac{a}{L} + \frac{b}{L^2} \right) ,$$

$$(12)$$

where Δ_∞, a, and b are fit parameters. We have chosen nine different energies $\hat{E}$ from the interval $[1000, 10\,000]$ and determined the corresponding saturation values $\Delta_\infty(\hat{E})$ using the fit (12). Fitting in turn the asymptotic behavior (11) to these values we obtained for the constant $C = -0.048$ in the odd and $C = -0.052$ in the even case. The results of the saturation values together with the asymptotic curve (11) are represented for the odd case in Fig. 8. Notice that the values obtained for the constant C deviate from the simple estimate using only the shortest periodic orbit. Another interesting aspect which can be deduced from Eq. (10) is that there exists a simple relation between the two saturation values [36]

$$\Sigma_\infty^2 = 2\Delta_\infty .$$

$$(13)$$

This relation is confirmed by our numerical data within the expected errors, see Table I, except at $\hat{E} = 10\,000$ in the even case.
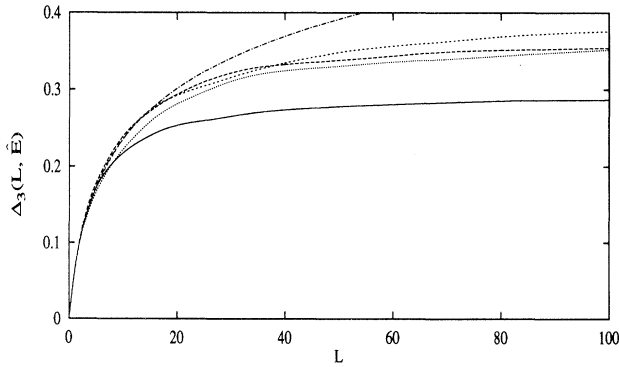

FIG. 7. Rigidity $\Delta_3(L, \hat{E})$ for even symmetry at different energies $\hat{E}$: $\hat{E} = 1000$ (full line), 4000 (long dashed), 7000 (short dashed), 10 000 (dots); $\delta = 1800$. The dashed-dotted line shows the expectation of random-matrix theory in the GOE case $\Delta_3^{\mathrm{GOE}}(L)$.
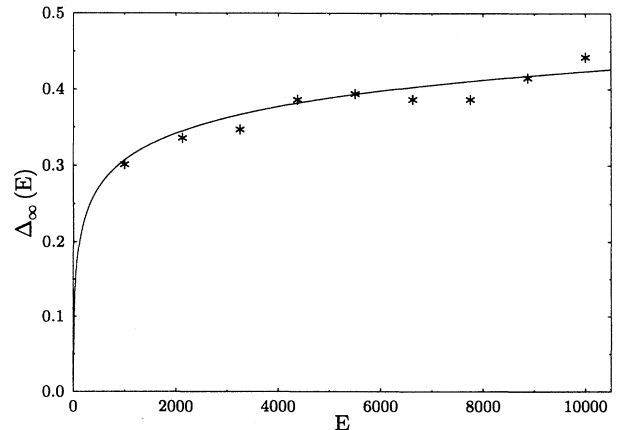

FIG. 8. Saturation values $\Delta_\infty(E)$ (stars) for odd symmetry at different energies, and the asymptotic curve (11) with $C = -0.048$ (full line).
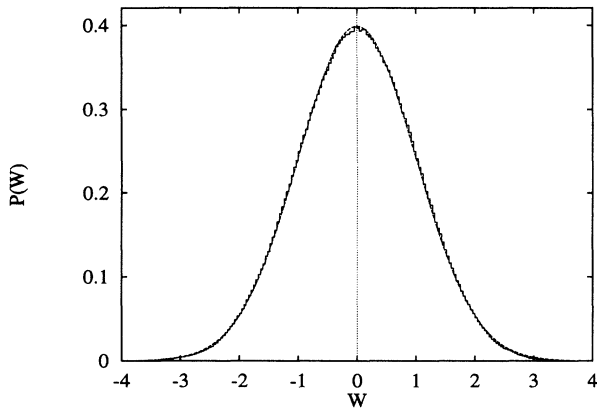
FIG. 9. Histogram of the mode-fluctuation distribution $P(W)$ (odd case). Dashed line: Gaussian limit distribution.

FIG. 10. Cumulative mode-fluctuation distribution for the even case in comparison with the cumulative version of (15).

F. The mode-fluctuation distribution $P(W)$

As we have seen in the preceding sections, the agreement of the computed number variance and rigidity with the predictions of random-matrix theory holds only at small- and medium-range correlations. A novel quantity which can be used as an indicator of quantum chaos in spectra is the distribution $P(W)$ of the mode fluctuation $W(E)$ [5,6]. The function $W(E)$ is defined as the normalized fluctuations of the mode number $N(E)$ around the mean mode number $\bar{N}(E)$

$$W(E) := \frac{N(E) - \bar{N}(E)}{\sqrt{\Delta_\infty(E)}} = \frac{N_{\text{osc}}(E)}{\sqrt{\Delta_\infty(E)}} \ . \qquad (14)$$

By definition $N_{\text{osc}}(E)$ fluctuates around zero, see Fig. 3, and furthermore it can be shown [19] that the second moment of $N_{\text{osc}}(E)$ tends asymptotically to the saturation value $\Delta_\infty(E)$ of the rigidity.

In [5,6] the conjecture has been put forward that classically chaotic systems should display a universal Gaussian behavior in the semiclassical limit $E \to \infty$

$$P_{\text{Gauss}}(W) = \frac{1}{\sqrt{2\pi}} e^{-\frac{1}{2} W^2} \ , \qquad (15)$$

whereas classically integrable systems should display non-Gaussian distributions $P(W)$. Numerically the distribution function was calculated by randomly choosing 10^7 energy values $E \in [0, 11\,000]$ and determining the
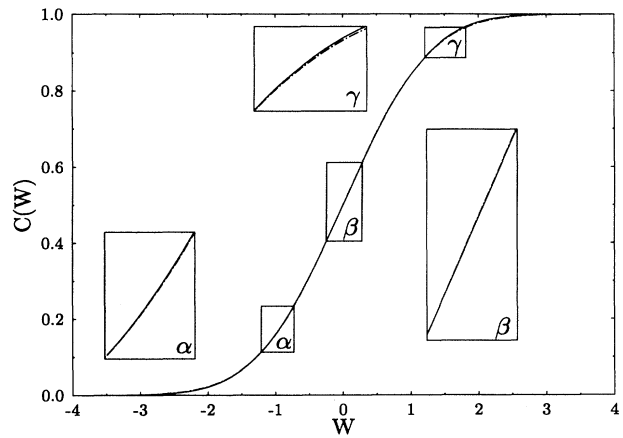
histogram of $W(E)$. As one can see in Fig. 9 the agreement between the histogram and the Gaussian normal distribution is very good. In Table II the mean value, variance, skewness, and kurtosis for the odd and even cases are shown. In order to quantify the visual impression, we applied the Kolmogorov-Smirnov test to the cumulative mode-fluctuation distribution $C(W)$ (see Fig. 10). We have chosen equidistantly 11 000 points of the unfolded energy interval $[0, 11\,000]$ and determined the maximum value D of the absolute difference between the cumulative distribution and the cumulative normal distribution. The significance level $\mathcal{P}$ of the distance D is in both symmetry cases above 60%, which strongly confirms the conjecture.

IV. THE TRACE OF THE COSINE-MODULATED HEAT KERNEL

It is well known that the Gutzwiller trace formula for bound quantum systems [12,1] obtained from a semiclassical approximation for the density of states is at best conditionally convergent. Based on Gutzwiller's semiclassical approximation for the level density a generalized trace formula has been derived by considering the trace $\text{Tr}\,[h(\hat{H}^{1/2})]$ of a suitable test function $h(p)$ of the square root of the Hamiltonian $\hat{H}$ [37]. The result obtained in the semiclassical limit of Planck's constant $\hbar \to 0$ is a periodic-orbit sum rule, which involves (in case of even Maslov indices) absolutely convergent sums and integrals

TABLE II. First moments of the mode-fluctuation distribution $P(W)$ for the odd and even case.

Moment	Odd symmetry	Even symmetry	Conjecture (15)
Average	−0.001	−0.003	0
Variance	0.992	0.996	1
Skewness	−0.021	0.008	0
Kurtosis	0.112	−0.089	0

only $(\hbar = 2m = 1)$

$$\sum_{n=1}^{\infty} h(p_n) \sim \int_0^{\infty} dp \, h(p) \bar{d}(p) + C \, h(0)$$
$$+ \sum_{\gamma} \sum_{k=1}^{\infty} \frac{l_{\gamma}}{\sqrt{|2 - \mathrm{Tr}M_{\gamma}^k|}} \mathcal{F}_{\gamma}\{h(kl_{\gamma})\} \ . \quad (16)$$

Here the sum on the left-hand side runs over all quantal eigenvalues (not unfolded) parametrized by the discrete momenta $\{p_n = \sqrt{E_n}\}$. The integral on the right-hand side is the so-called "zero-length contribution" and is completely determined by the generalized Weyl's law $\bar{d}(p) = \frac{d\bar{N}(p^2)}{dp}$. The γ summation runs over all primitive periodic orbits γ of length l_{γ}, whereas $\sum_k$ counts multiple traversals corresponding to periodic orbits of length kl_{γ}; M_{γ} is the monodromy matrix, C is the constant term in Weyl's law, and $\mathcal{F}_{\gamma}\{h(x)\}$ denotes the Fourier transform of the test function $h(p)$ (incorporating the phase shift due to the Maslov index)

$$\mathcal{F}_{\gamma}\{h(x)\} = \frac{1}{\pi} \int_0^{\infty} dp \, h(p) \, \cos(px - k\nu_{\gamma} \tfrac{\pi}{2}) \ , \quad (17)$$

where ν_{γ} denotes the Maslov index which is twice the number of reflections at Dirichlet boundaries plus the maximal number of conjugate points μ_{γ} (see, e.g., [38,39]).

Starting from the generalized trace formula (16) we can study the inverse problem of quantum chaos: to obtain the lengths of the periodic orbits from the quantal energy levels. This problem can be solved by considering the trace of the cosine-modulated heat kernel [40,41] $\mathrm{Tr}\{\cos[(-\Delta)^{1/2}L] e^{t\Delta}\}$, which is obtained from Eq. (16) by choosing the following test function:

$$h(p) = \cos(pL) e^{-p^2 t}; \qquad p = \sqrt{E} \ , \quad t > 0 \ . \quad (18)$$

Due to the geometry of the cardioid billiard with its focusing boundary, the orbits listed in Table III have a nonvanishing maximal number of conjugate points μ_{γ}. Thus ν_{γ} can be odd or even which results in a sine- or cosine-Fourier transform respectively. For even $k\nu_{\gamma} = 2m$ one has a cosine-Fourier transform which yields for (18)

$$\mathcal{F}_{\gamma}\{h(x)\} = \frac{(-1)^m}{4} \frac{1}{\sqrt{\pi t}} \left[\exp\left(-\frac{(x-L)^2}{4t}\right) + \exp\left(-\frac{(x+L)^2}{4t}\right) \right] \ , \quad (19)$$

whereas for odd $k\nu_{\gamma} = 2m + 1$ the result of the sine-Fourier transform of (18) is given by

$$\mathcal{F}_{\gamma}\{h(x)\} = \frac{(-1)^m}{4} \frac{1}{\pi t} \left[(x-L) \, {}_1F_1\left(1, \frac{3}{2}, -\frac{(x-L)^2}{4t}\right) + (x+L) \, {}_1F_1\left(1, \frac{3}{2}, -\frac{(x+L)^2}{4t}\right) \right] \ , \quad (20)$$

where ${}_1F_1(a, b, z)$ is Kummer's function. The Fourier transforms (19) and (20) clearly display the different kind of shapes of the periodic-orbit contributions to the trace formula as a function of L for fixed t. If $k\nu_{\gamma}$ is even, one obtains a Gaussian peak at $L = kl_{\gamma}$, whereas for odd $k\nu_{\gamma}$ one has a zero at the lengths of the periodic orbits because ${}_1F_1(1, \frac{3}{2}, 0) = 1$. This is similar to the observation made by Sieber et al. [42] in the case of the Fourier analysis of the spectrum.

The trace of the cosine-modulated heat kernel allows one to extract the length and stability of the first orbits and even the value of $k\nu_{\gamma}$ modulo 4. The last property cannot be read off in the case of the often considered so-called power spectrum $D(x) = \left| \int_0^{p_{max}} dp \, e^{ipx} [d(p) - \bar{d}(p)] \right|^2$.

With the first 11 000 levels and a smoothing parameter $t = 0.0001$ we obtained the graph (full line) shown in Fig. 11 for the odd symmetry case. For a proper comparison with the trace formula, we have to subtract from the right-hand side of (16) the contribution of the unknown part of the energy spectrum, $\{E_n; n > N = 11\,000\}$. This contribution is estimated by first replacing the sum over the discrete spectrum by a Riemann-Stieltjes integral, and then approximating the integral by means of Weyl's law, Eqs. (3) or (4):

$$\sum_{n=N+1}^{\infty} h(p_n) = \int_{E_N}^{\infty} dN(E) \, h(\sqrt{E}) \approx \int_{\sqrt{E_N}}^{\infty} dp \, h(p) \bar{d}(p) \ .$$

Subtracting this term from the right-hand side of (16) implies that the integration in the integral in (16) has to be restricted to the interval $[0, \sqrt{E_N}]$. With this approx-

TABLE III. Dynamical data of the first primitive periodic orbits. l_{γ} is the length of the orbit γ, $\mathrm{Tr}M_{\gamma}$ denotes the trace of the monodromy matrix, μ_{γ} is the maximal number of conjugate points, and ν_{γ} is the Maslov index [for odd (D) and even (N) symmetry].

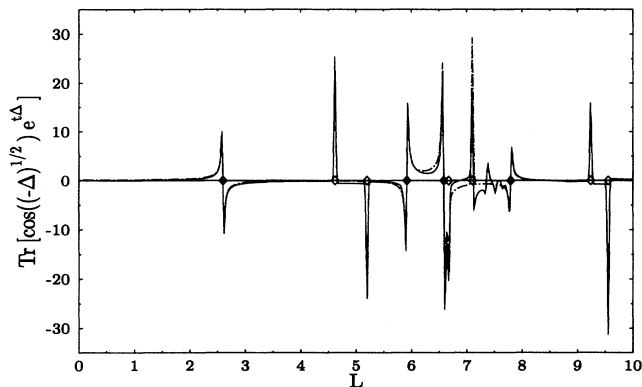| Orbit no.	l_{γ}	$\mathrm{Tr}\,M_{\gamma}$	μ_{γ}	ν_{γ} (D)	ν_{γ} (N)
1	2.598	−2.50	1	5	3
2	4.618	−4.40	2	8	6
3	5.918	−9.74	3	11	9
4	6.585	7.62	3	13	9
5	6.673	−28.36	4	14	12
6	7.103	12.45	4	16	12
7	9.552	−16.31	4	18	12

FIG. 11. Trace of the cosine-modulated heat kernel for odd symmetry with $t = 0.0001$. Full line: sum over the first 11 000 energy levels; dashed line: periodic-orbit sum. The squares indicate the lengths l_γ of the first periodic orbits, see Table III and Fig. 12, and of their repetitions.

FIG. 12. Primitive periodic orbits with $l_\gamma < 10$. Notice that orbit no. 5 does not run into the cusp.

imation we also show in Fig. 11 the right-hand side of (16) (dashed line) by using the geometrical data of the primitive periodic orbits known so far (see Table III and Fig. 12). We observe a striking agreement between both graphs which indicates the accuracy of the computed energy levels. Notice the excellent resolution of the two peaks near $L \approx 6.6$ which correspond to orbits no. 4 and no. 5.

In the interval $L \in [7.1, 7.6]$ there are some differences between the trace of the cosine-modulated heat kernel calculated from the eigenvalues and the periodic-orbit sum, respectively, which are probably caused by orbits which run into the cusp of the cardioid billiard. Their contribution is expected to be of higher order in $\hbar$ and thus is not included in the trace formula (16). Similar differences exist in the even symmetry case. A detailed analysis of the periodic-orbit theory for the cardioid billiard is in progress and will be presented separately.

V. SUMMARY AND DISCUSSION

In this paper we have presented a detailed analysis of the spectral statistics of the cardioid billiard. This dynamical system is strongly chaotic and thus constitutes an ideal testing ground for quantum chaology. It is found that the level-spacing distribution is in very good agreement with the Wigner distribution. However, the number variance and rigidity clearly violate the universal laws of random-matrix theory for medium and large correlation lengths. The observed nonuniversal behavior agrees with semiclassical expectations. Our results thus further strengthen the evidence accumulated so far showing that the applicability of the random-matrix model is limited to short-range correlations only.

A promising candidate for a universal measure of quantum chaos in spectra is the mode-fluctuation distribution $P(W)$. We have shown in Sec. III F that this novel spectral st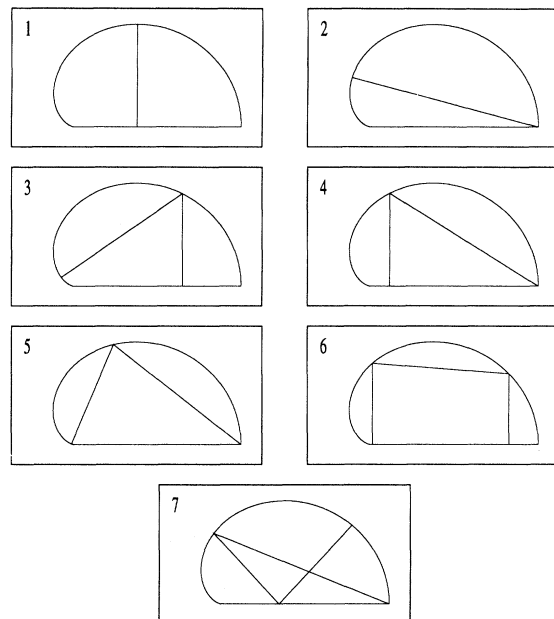atistic indeed displays at a high significance level a universal Gaussian behavior in agreement with a recent conjecture. In view of this result it appears even more urgent to inquire for a rigorous derivation of the conjecture from first principles.

Finally, in Sec. IV, we have studied the trace of the cosine-modulated heat kernel and have compared it with the theoretical result derived from Gutzwiller's semiclassical trace formula. The overall agreement between "experiment" and theory is striking. It is amazing to see in Fig. 11, for instance, the pronounced zero at the location of the length of the shortest periodic orbit. The observed structure follows precisely the theoretical curve as described by Eq. (20). This is a nice illustration of "inverse quantum chaology:" Knowing the quantal eigenvalues we are able to determine not only the lengths of classical periodic orbits, but also whether they possess conjugate points or not. This agreement with periodic-orbit theory calls for a more elaborate investigation of the trace formula in the case of the quantized cardioid billiard. Work along this line is in progress and will be presented later.

ACKNOWLEDGMENTS

[1] M.C. Gutzwiller, *Chaos in Classical and Quantum Mechanics* (Springer, New York, 1990).

[2] M.V. Berry, J. Phys. A **10**, 2083 (1977).

[3] R. Aurich and F. Steiner, Physica D **64**, 185 (1993).

[4] B. Li and M. Robnik, J. Phys. A **27**, 5509 (1994).

[5] F. Steiner, in *Schlaglichter der Forschung. Zum 75. Jahrestag der Universität Hamburg 1994*, edited by R. Ansorge, Festschrift published on the occasion of the 75th anniversary of the University of Hamburg (Dietrich Reimer Verlag, Berlin, 1994), pp. 543–564.

[6] R. Aurich, J. Bolte, and F. Steiner, Phys. Rev. Lett. **73**, 1356 (1994).

[7] M.V. Berry and M. Tabor, Proc. R. Soc. London Ser. A **356**, 375 (1977).

[8] O. Bohigas, M.-J. Giannoni, and C. Schmit, Phys. Rev. Lett. **52**, 1 (1984).

[9] *Statistical Theories of Spectra: Fluctuations*, edited by C.E. Porter (Academic Press, New York, 1965).

[10] M.L. Mehta, *Random Matrices*, revised and enlarged 2nd ed. (Academic Press, San Diego, 1991).

[11] *Chaos and Quantum Physics*, Proceedings of the Les Houches Summer School of Theoretical Physics, Les Houches, 1989, edited by M.-J. Giannoni, A. Voros, and J. Zinn-Justin (Elsevier, Amsterdam, 1991).

[12] M. C. Gutzwiller, J. Math. Phys. **12**, 343 (1971).

[13] M.V. Berry, Proc. R. Soc. London Ser. A **400**, 229 (1985).

[14] M.V. Berry, Nonlinearity **1**, 399 (1988).

[15] M.V. Berry, *Chaos and Quantum Physics* [11], pp. 251–303.

[16] R. Aurich and F. Steiner, Physica D **82**, 266 (1995).

[17] R. Aurich, F. Scheffler, and F. Steiner, Phys. Rev. E. **51**, 4173 (1995).

[18] J. Bolte, G. Steil, and F. Steiner, Phys. Rev. Lett. **69**, 2188 (1992).

[19] J. Bolte, Int. J. Mod. Phys. B **7**, 4451 (1993).

[20] M. Robnik, J. Phys. A **16**, 3971 (1983).

[20] M. Robnik, J. Phys. A **16**, 3971 (1983).

[21] M. Wojtkowski, Commun. Math. Phys. **105**, 391 (1986).

[22] D. Szász, Commun. Math. Phys. **145**, 595 (1992).

[23] R. Markarian, Nonlinearity **6**, 819 (1993).

[24] N.I. Chernov and C. Haskell, 1994 (unpublished).

[25] Ya.G. Sinai, Sov. Math. Dokl. **4**, 1818 (1963).

[26] Ya.G. Sinai, Russian Math. Surveys **35**, 137 (1970).

[27] L.A. Bunimovich, Funct. Anal. Appl. **8**, 73 (1974).

[28] L.A. Bunimovich, Commun. Math. Phys. **65**, 295 (1979).

[29] L.A. Bunimovich and Ya. G. Sinai, Commun. Math. Phys. **78**, 247 (1980).

[30] L.A. Bunimovich and Ya. G. Sinai, Commun. Math. Phys. **78**, 479 (1981).

[31] H.P. Baltes and E.R. Hilf, *Spectra of Finite Systems* (Bibliographisches Institut, Mannheim, 1976).

[32] T. Prosen and M. Robnik (private communication).

[33] M. Robnik, J. Phys. A **17**, 1049 (1984).

[34] T. Prosen and M. Robnik, J. Phys. A **26**, 2371 (1993).

[35] Here the value of the spectral staircase function (2) at an unfolded eigenvalue E_n is defined as

$$N(E_n) = \lim_{\epsilon \to 0} \left(\frac{N(E_n - \epsilon) + N(E_n + \epsilon)}{2} \right) = n - \tfrac{1}{2} \ .$$

[36] R. Aurich and F. Steiner, Physica D **43**, 155 (1990).

[37] M. Sieber and F. Steiner, Phys. Lett. A **144**, 159 (1990).

[38] S.C. Creagh, J.M. Robbins, and R.G. Littlejohn, Phys. Rev. A **42**, 1907 (1990).

[39] M. Sieber, Ph.D. thesis, Universität Hamburg, DESY Report No. DESY 91-030, 1991 (unpublished).

[40] R. Aurich, M. Sieber, and F. Steiner, Phys. Rev. Lett. **61**, 483 (1988).

[41] R. Aurich and F. Steiner, Phys. Rev. A **45**, 583 (1992).

[42] M. Sieber, U. Smilansky, S. C. Creagh, and R. G. Littlejohn, J. Phys. A **16**, 6217 (1993).